Geophysical Research Letters

RESEARCH LETTER
10.1029/2022GL098187

Impact of Rainfall on Tropical Cyclone-Induced Sea Surface Cooling

Karthik Balaguru[1], Gregory R. Foltz[2], L. Ruby Leung[1], and Samson M. Hagos[1]

[1]Pacific Northwest National Laboratory, Richland, WA, USA, [2]NOAA/Atlantic Oceanographic and Meteorological Laboratory, Miami, FL, USA

Key Points:

- Analysis of a suite of observations suggests that high rain rates can reduce the sea surface cooling induced by weak tropical cyclones (TCs)
- Consistent results are obtained from high-resolution climate model simulations and sensitivity experiments with an ocean mixed layer model
- Changes in upper-ocean stratification and mixing are primarily responsible for the rainfall effect on TC-induced sea surface temperature cooling

Supporting Information:

Supporting Information may be found in the online version of this article.

Correspondence to:

K. Balaguru,
Karthik.Balaguru@pnnl.gov

Citation:

Balaguru, K., Foltz, G. R., Leung, L. R., & Hagos, S. M. (2022). Impact of rainfall on tropical cyclone-induced sea surface cooling. *Geophysical Research Letters*, *49*, e2022GL098187. https://doi.org/10.1029/2022GL098187

Received 3 FEB 2022
Accepted 28 APR 2022

Abstract Tropical cyclones (TCs) are often accompanied by strong winds and torrential rains. While the winds associated with TCs tend to enhance mixing in the upper ocean, the freshwater input from rain can stratify the water column and limit mixing. However, the extent to which the stabilizing effect of rainfall can compete with wind-induced mixing and to what degree it modulates TC-induced sea surface cooling remain unknown. Here we show, using a suite of observations, that heavy rains under weak TCs can significantly reduce the magnitude of cold wakes induced by them. When compared to storms with low rain rates, the ocean surface under TCs with high rain rates freshens significantly and cools less. High-resolution climate model simulations and idealized experiments with an ocean mixed layer model support these results and reveal that oceanic mixing processes are primarily responsible for reduced cooling under TCs, with a lesser role for surface fluxes.

Plain Language Summary Strong winds of tropical cyclones (TCs) induce substantial mixing in the upper ocean, a process that entrains colder deeper water into the mixed layer resulting in cooling of the sea surface temperature (SST). Hence, ocean density stratification plays a crucial role in the SST response to TCs and consequently, in their intensification. While most previous studies considered the role of prestorm stratification near the ocean surface on TC-induced SST cooling, the role of rainfall from TCs in the SST response to storms has mostly remained unexplored. In this study, using a variety of observations, we show that the SST cooling is reduced significantly for weak TCs with large rain rates. Under high rain rates, the upper ocean freshens considerably and the salinity stratification is enhanced. Consequently, vertical mixing and the entrainment of subsurface water is reduced, and the SST cooling decreases. Similar results are obtained using high-resolution simulations based on the Energy Exascale Earth System Model. Finally, a set of idealized numerical sensitivity experiments with the Price-Weller-Pinkel ocean mixed layer model confirm the role of vertical ocean mixing in the rainfall effect on TC-induced SST change. These results have potential implications for improving our understanding of TC-ocean interactions.

1. Introduction

Tropical cyclones (TCs) intensify by extracting heat energy from the ocean surface (K. A. Emanuel, 1986), making the sea surface temperature (SST) under storms, and the processes governing its evolution, crucial for storm development (Bender & Ginis, 2000; Cione & Uhlhorn, 2003; DeMaria & Kaplan, 1994; Holland, 1997; K. A. Emanuel, 1999). In the open ocean, changes in SST under TCs mainly result from a balance between the momentum flux of the storm and turbulent mixing in the upper ocean, while surface heat fluxes play a more important role in shallow coastal areas (Morey et al., 2006; Shen & Ginis, 2003). Strong TC winds cause significant mixing, which entrains cooler deeper water into the surface mixed layer (D'Asaro et al., 2007; Price, 1981), a process that lowers SST and acts as a negative feedback on the storm's intensity (Bender & Ginis, 2000; Cione & Uhlhorn, 2003; K. Emanuel et al., 2004; K. A. Emanuel, 1999; Schade & Emanuel, 1999). Since mixing is strongly dependent on the vertical density structure, upper-ocean stratification and processes that affect it play an important role in the SST response to TCs (Price, 1981).

Past work on the impacts of ocean stratification on TC-induced SST cooling has predominantly considered prestorm stratification (Balaguru et al., 2015; Korty et al., 2008; I.-I. Lin et al., 2013; Price, 2009; Vincent et al., 2012; Vincent et al., 2014). For instance, weak vertical temperature gradients in regions with a deep thermocline favor the intensification of TCs through reduced SST cooling and enhanced heat flux at the ocean surface (I. Lin et al., 2005; Mainelli et al., 2008; Shay et al., 2000). Similarly, fresh water outflow from major

river systems tends to strengthen storms through a reduction in oceanic mixing and sea surface cooling (Balaguru et al., 2012; Balaguru, Foltz, et al., 2020; Grodsky et al., 2012; Hlywiak & Nolan, 2019; Reul et al., 2014; Rudzin et al., 2019, 2018). However, the influence of TC precipitation on TC wind-induced SST cooling, through coincidental changes in salinity stratification, remains largely unknown. Using an analysis of observations, Jourdain et al. (2013) suggested that TC rainfall reduces TC-induced SST cooling by a small but nonnegligible amount on average. However, their analysis is based on a simple analytical model of the upper-ocean SST response to TCs. Subsequently, modeling efforts using case studies of individual TCs found appreciable reduction in TC cold wakes due to TC rainfall (Liu et al., 2020; Steffen & Bourassa, 2020). Here, we address this question using a suite of observations, high-resolution climate model simulations, and numerical experiments with an ocean mixed layer model.

2. Data, Models, and Methods

2.1. Data and Coupled Climate Model

TC track data are obtained from the International Best Track Archive for Climate Stewardship (Knapp et al., 2010) at https://www.ncdc.noaa.gov/ibtracs/. Daily precipitation from the Global Precipitation Climatology Project (GPCP) version 1.3 (Huffman et al., 2001) at a horizontal resolution of 1°, obtained from https://www.ncei.noaa.gov/products/climate-data-records/precipitation-gpcp-daily, is used to estimate precipitation along TC tracks. NOAA daily optimum interpolation (OI) SST data version 2.1 (Reynolds et al., 2007) at a horizontal spatial resolution of 0.25°, obtained from https://www.ncdc.noaa.gov/oisst, are used to estimate prestorm SSTs and SST change under TCs. The NOAA OI SST product assimilates in situ measurements along with data from the Advanced Very High Resolution Radiometer infrared sensor. 5-day mean vertical profiles of ocean temperature and salinity from the Simple Ocean Data Assimilation version 3.3.1 (SODA3) (Carton et al., 2018), an eddy-permitting ocean reanalysis obtained from https://www.soda.umd.edu/, are used to estimate prestorm mixed layer depth (MLD), upper-ocean temperature stratification, sea surface salinity (SSS), and the change in SSS induced by TCs. These data are available at a spatial resolution of 0.5°. All data are obtained for the 12-year period, 2004–2015. We use data beginning in 2004 since estimates of the upper-ocean state are more reliable with near-global coverage of Argo floats (Roemmich et al., 2009). The length of the analysis period is constrained by the availability of SODA3.

In addition to the AVHRR-based NOAA OI SST data, we also obtain daily maps of SST at 0.25° spatial resolution from the Tropical Rainfall Measuring Mission (TRMM) Microwave Imager (TMI) (Gentemann et al., 2004). These data are available for download from https://www.remss.com/missions/tmi/. Unlike infrared sensors, microwave sensors can see better through clouds and may provide improved estimates of TC-induced SST cooling (Wentz et al., 2000). TMI SST data are obtained for the period from 2004 to 2014, since the TMI sensor became inoperable in 2015. Similarly, 3-hourly precipitation from the TRMM Multisatellite Precipitation Analysis version 7 at a horizontal spatial resolution of 0.25° is obtained from https://disc.gsfc.nasa.gov/datasets/TRMM_3B42_7/summary for the period 2004–2014. These data are used to understand the sensitivity of our main results to various data sources.

To support our results based on observations, we use 20 years of simulations based on the high-resolution configuration of the Energy Exascale Earth System Model (E3SM) version 1 (Caldwell et al., 2019). The atmospheric component of the model has a spatial resolution of about 25 km with 72 vertical levels. The ocean component, which has 80 vertical levels, has an eddy-resolving grid spacing that varies from 18 km in the tropics to about 6 km near the poles. The simulation is forced by time-invariant 1950s forcing following the High Resolution Model Intercomparison Project (Haarsma et al., 2016) protocol. TC tracks in the model simulations are generated using Tempest Extremes, a scale-aware feature tracking algorithm (Ullrich & Zarzycki, 2017). The model produces a reasonable distribution of TCs and simulates TC-ocean interactions realistically (Balaguru, Leung, et al., 2020). For further details regarding the model and its simulation of TCs, see Caldwell et al. (2019) and Balaguru, Leung, et al. (2020), respectively. For more information about the implementation of Tempest Extremes in E3SM, see Balaguru, Leung, et al. (2020).

2.2. Methods

Climatological maps of TC rainfall, and TC-induced SSS and SST changes, are used to broadly understand the relationship between rainfall and the upper-ocean response to TCs. We first follow TC tracks and compute the various parameters. Next, for each parameter, we generate the accumulated value over the entire analysis period (2004–2015) at each grid point. Finally, division by the total number of years (12) gives the climatological response, which is the average value per TC-season for the parameter.

We perform a Lagrangian composite analysis to estimate the impact of TC rainfall on TC-induced SST cooling. First, following TC tracks, we estimate the TC initial intensity, translation speed, rain rate, prestorm SST, prestorm SSS, prestorm temperature stratification, prestorm MLD (computed based on a density threshold of 0.05 kg m^{-3}), SST change, and SSS change. Using SODA3 5-day mean data, prestorm temperature stratification (TSTRAT, defined as the temperature difference over the upper 100 m), MLD, and SSS are estimated as the values averaged over the 5-day period preceding the storm's arrival. Similarly using SODA3 data, SSS change is estimated as the difference in SSS averaged over the 5-day period following the TC's arrival and the prestorm SSS. Using daily NOAA OI SST data, SST change is estimated as the difference between SST on the day of the storm and SST 2 days before the storm's arrival. For daily GPCP rainfall, we use data from the calendar day of each TC's location, while for TRMM, we use the 3-hr data that is closest to the hour of the TC's passage.

To determine the role of TC rainfall on TC-induced SST cooling, first we divide the data into two sets: (a) one for which the rain rates exceed the 90th percentile of the TC rain rate distribution and termed the "wet" case, and (b) one for which the rain rates are below the 10th percentile of the TC rain rate distribution and termed the "dry" case. Next, we subsample data to ensure that the distributions of storm state and prestorm ocean initial conditions are statistically similar for the two sets to remove the impacts of confounding factors. We then examine mean differences in SST change and SSS change between the two sets of data, which are attributed to TC rainfall. Considering that the average TC radius of maximum winds is about 50 km (Hsu & Yan, 1998), all parameters are averaged over a $2° \times 2°$ box centered on the storm to account for variability in the areal extent of SST cooling and the asymmetry in their spatial distribution (Balaguru et al., 2015). Also, this accounts for resolution differences among the various observational data sets used in our study. Note that the area-averages of sea surface cooling are likely to be dominated by values at the radius of maximum winds, where the signal tends to be strongest.

A similar analysis is conducted using E3SM, except that all ocean parameters are based on daily model output. In addition to the parameters mentioned for the observational analysis, we compute air-sea fluxes at the ocean surface in E3SM to more clearly understand the role of surface fluxes in the modulation of the SST response to TC rainfall. We also use ocean MLDs (computed based on a density threshold of 0.03 kg m^{-3}) near the cores of storms, where maximum mixing tends to occur, to explore the influence of TC rainfall on oceanic mixing. While we use the 90th and 10th percentile of rain rates as thresholds for the "wet" and "dry" cases in the observational analysis, we use values close to the 75th and 25th percentile as thresholds, respectively, for the E3SM-based analysis. This is the maximum possible gap in rain rates between the "wet" and "dry" cases that ensures a statistically similar distribution of storm state and prestorm ocean conditions in the simulation. Probability distribution functions (PDFs) of MLD change induced by TCs are estimated using the Monte Carlo technique of repeated random sampling. For each parameter, we randomly select half of the values and produce a distribution. We then repeat this process a hundred times. For each range of values, the mean and standard deviation across the distributions gives the corresponding bar height and error, respectively.

2.3. Ocean Model Experiments

To further explore the role of oceanic mixing in the rain-induced modulation of the SST response to TCs, we performed idealized numerical experiments using the Price-Weller-Pinkel (PWP) one-dimensional ocean mixed layer model (Price et al., 1986). The model was initialized with constant salinity of 34.5 psu and a temperature profile that is consistent with the average initial MLD (25 m) and temperature stratification (0.08°C m^{-1}) obtained from the observational analysis. We subject the ocean profiles to idealized TC winds assuming that the surface wind field is axisymmetric with the wind speed, a function of the storm's intensity (based on the mean observed maximum wind speed of 40 kt), radius of maximum winds (assumed to be 50 km), and distance from the storm's center (DeMaria, 1987). In our case, the perpendicular distance from the storm center is zero (i.e., a transect through the center of the TC), which results in a single wind profile in which the wind magnitude

is simply a function of time. The time duration for which the wind forcing is applied is based on the average observed TC translation speed of 5.8 m s^{-1}. All components of the surface heat flux are set to zero throughout the model runs. For further details regarding the choice of various parameters and the experimental design, see Balaguru et al. (2015). We perform two sets of simulations: a "Rain" simulation in which the TC forcing includes a maximum storm rainfall rate of 15 mm hr^{-1}, corresponding to the average maximum rain rate based on observations and a "No rain" simulation in which the TC forcing does not include rainfall. For the "Rain" simulation, the maximum rainfall rate occurs at the radius of maximum wind and decreases radially as a function of wind speed, giving 24-hr accumulated rainfall of 220 mm, centered on the storm. The difference between the "Rain" and "No rain" simulations represents the effect of TC-induced rainfall on oceanic mixing and consequently, SST for TCs that produce heavy rain.

3. Results

We begin by examining the climatological global distributions of TC rainfall and the upper-ocean salinity and temperature responses to TCs (Figure 1). The distribution of rainfall due to TCs, based on GPCP daily rainfall data, shows that TCs produce significant rain over the global tropical and subtropical oceans (Figure 1a). Highest values are found in the northwest Pacific, east Pacific, and to some extent in the southwest Indian Ocean, collocated with the areas of highest TC track density (Bell et al., 2013) and warm SSTs that promote convection and TC rainfall (Y. Lin et al., 2015). These results are consistent with past estimates (W. Zhang et al., 2021). The SODA3 ocean reanalysis-based SSS response to TCs (Figure 1b), generated from the Lagrangian analysis, is in general agreement with the TC rainfall climatology. Broadly, surface salinification tends to occur in regions with less TC rainfall and strong vertical salinity gradients (Figure S1 in Supporting Information S1), such as in areas dominated by plumes of large river systems. These regions include the Bay of Bengal in the northern Indian Ocean, the South China Sea, and the tropical North Atlantic Ocean (Balaguru et al., 2012; Grodsky et al., 2012; Reul et al., 2021; Zeng & Wang, 2017). Also included is the southwest Pacific, which receives significant precipitation from the South Pacific Convergence Zone. On the contrary, surface freshening occurs in regions with significant TC rainfall and weak vertical salinity gradients (Figure S1 in Supporting Information S1), such as in the eastern Pacific, northwestern Pacific away from the east Asian coastline, and in the South Indian ocean basins. Note that in the eastern Pacific, strong upper-ocean salinity stratification is found only near the southern edge of the basin, with low salinity stratification in much of the basin.

The climatological SST response to TCs (Figure 1c), based on NOAA OI SST, is in broad agreement with the climatological TC track density (Bell et al., 2013). Largest annual mean TC-induced decreases in SST occur in the eastern Pacific, likely due to high TC track densities (Bell et al., 2013) and a shallow thermocline (Balaguru et al., 2013). Strong sea surface cooling is also found in the northwest Pacific and in the southwest Indian Ocean region near Madagascar. As mentioned earlier, the SST change under TCs plays a critical role in their intensification. Thus, one wonders whether TC-induced changes in ocean salinity (Figure 1b), which result from an interplay of TC rainfall and prestorm ocean stratification, can modulate the SST response to TCs. To address this, we perform a Lagrangian composite analysis of TC-induced changes in the upper ocean using a combination of observations and numerical model simulations.

At a given location, rainfall from TCs is highly dependent on the initial storm state. For instance, using GPCP data, we find that the correlation between TC rain rate and TC intensity is about 0.4 and the correlation between TC rain rate and TC translation speed is about −0.2. Both values are highly significant considering a sample size of nearly 14,000. In other words, stronger- and slower-moving storms tend to rain more at a given location. However, the impact of storm state on sea surface cooling is also well-known, with slow-moving and intense storms causing more SST cooling (Price, 1981). To remove the effects of storm state on the TC rainfall influence on SST cooling, we subsample the data to ensure that the TC intensity and translation speed are statistically similar in the "wet" and "dry" samples used for comparison. Also, to remove the influence of prestorm ocean state, we further subsample the data to ensure that the initial upper-ocean conditions are statistically similar. The results from this analysis are shown in Table 1. Due to the sampling constraints in our analysis, we are only able to consider weak TCs with an average wind speed of about 40 kt.

The area-averaged rain rate for the "wet" case is about 54 mm day^{-1}, nearly 50 mm day^{-1} higher than for the "dry" case. As a result, the surface freshens significantly. Relative to the "dry" case, the area-averaged SSS decreases by

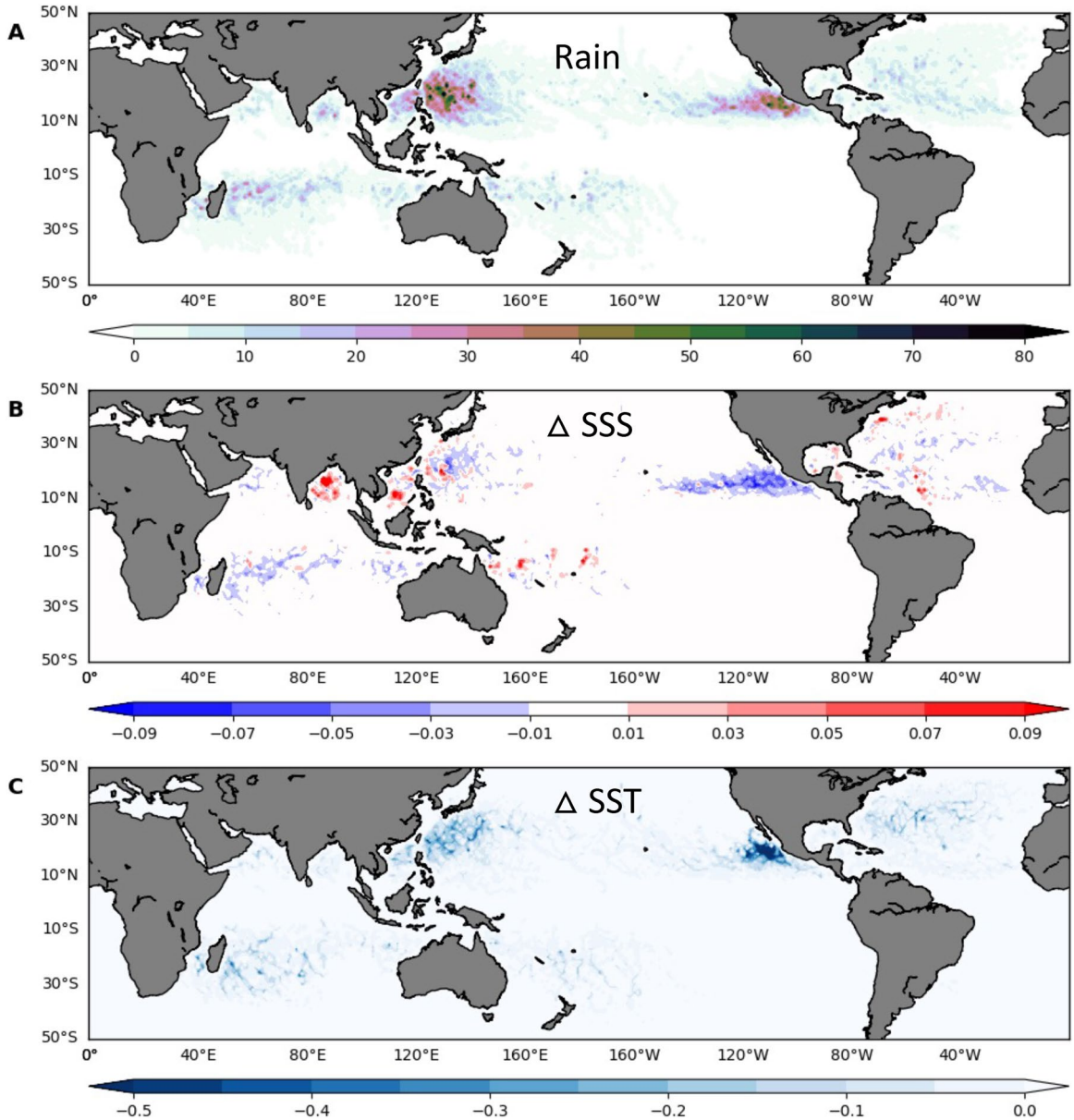

Figure 1. Climatological tropical cyclone (TC)-season mean (a) rainfall from TCs (mm day^{-1}), (b) sea surface salinity (SSS) (psu) response to TCs, and (c) sea surface temperature (SST) (°C) response to TCs. Rainfall is based on Global Precipitation Climatology Project daily data, SSS is based on 5-day mean Simple Ocean Data Assimilation version 3.3.1 ocean reanalysis data, and SST is based on NOAA optimum interpolation SST daily data. The period of analysis is 2004–2015.

about 0.1 psu in the "wet" case. More importantly, the area-averaged SST cooling decreases by about 0.26°C for the "wet" case compared to the "dry" case. To verify these results that are derived from AVHRR-based NOAA OI SST and GPCP rainfall, we performed a similar analysis using SST and rainfall data from TRMM (Table S1 in Supporting Information S1). The mean area-averaged rain rates for the "wet" and "dry" cases are about 5.8 mm hr^{-1} and 0.3 mm hr^{-1}, respectively, indicating a difference of about 5.5 mm hr^{-1}. Relative to the "dry" case, the SSS decreases in the "wet" case by about 0.05 psu. Further, the magnitude of SST cooling decreases by about 0.43°C for the "wet" case compared to the "dry" case, suggesting that these results are in broad agreement with those obtained earlier.

The observational analysis suggests that for weak TCs, sea surface cooling is reduced for TCs with large rain rates. To further understand how rainfall from TCs modulates the upper-ocean response to them, we analyzed high-resolution E3SM simulations by performing a Lagrangian composite analysis along model TC tracks. As

Table 1
Lagrangian Composite Analysis of Tropical Cyclone (TC) Rainfall Impacts on TC-Induced Sea Surface Temperature (SST) Cooling Using TC Track Data, NOAA Optimum Interpolation SST v2, Simple Ocean Data Assimilation Version 3.3.1 Ocean Reanalysis, and Global Precipitation Climatology Project Rainfall Data for the Period 2004–2015

Parameter	Wet	Dry	Difference
Maximum wind speed (kt)	40.5 ± 5.7	38.6 ± 4.9	1.9
Translation speed (m s^{-1})	5.9 ± 2.2	5.9 ± 1.4	0.0
Rain (mm day^{-1})	54.1 ± 5.0	5.0 ± 2.2	**49.1**
Prestorm TSTRAT (°C)	−5.2 ± 0.9	−5.6 ± 1.2	0.4
Prestorm MLD (m)	25.5 ± 14.3	26.0 ± 11.0	−0.5
Prestorm SST (°C)	27.4 ± 0.6	27.4 ± 0.5	−0.1
Prestorm SSS (psu)	34.7 ± 0.2	34.5 ± 0.5	0.2
SSS change (psu)	−0.10 ± 0.06	−0.00 ± 0.1	**−0.10**
SST change (°C)	0.05 ± 0.15	−0.21 ± 0.46	**0.26**

Note. The "Wet" column corresponds to those TCs with high rain rates, "Dry" column corresponds to those TCs with low rain rates, and "Difference" represents the difference between the "Wet" and "Dry" sets. For each parameter, the mean value along with the error, which is represented by the standard deviation, is shown. For the "Difference" column, the values in bold indicate statistical significance at the 5% level. Data here have been subsampled to ensure that the initial storm state and prestorm ocean conditions are statistically similar for the "Wet" and "Dry" sample sets.

in observations, subsampled model TC distributions have an average maximum wind speed of about 40 kt. The climatological upper-ocean temperature response to TCs is well-simulated in the model compared to observations (Balaguru, Leung, et al., 2020). After the arrival of the TC, the sea surface starts cooling with the lifting of the thermocline and the entrainment of cooler subsurface waters (Figure 2a). The mean rain rate for the "wet" case is about 6.1 mm hr^{-1} and for the "dry" case it is about 1.3 mm hr^{-1}. As a result of the additional rainfall, the sea surface freshens considerably in the "wet" case, by about 0.06 psu compared to the "dry" case. The most significant freshening is approximately confined to a depth of 10 m on the day of the TC, and it is subsequently mixed deeper (Figure 2b). In response to the rainfall-induced increase in salinity stratification, SST and upper-ocean cooling are reduced in the "wet" case relative to the "dry" case (Figure 2c). While the mean SST change in the "dry" case is about −0.28°C, the mean SST change in the "wet" case is −0.16°C.

Although SST changes under TCs are primarily caused by oceanic mixing and upwelling, some influence from surface fluxes may also be possible (H. Zhang et al., 2021), especially considering that the results are based on weaker storms. To address this, we examine air-sea fluxes under TCs. The net heat flux for the "wet" case is about −65 Wm^{-2} and for the "dry" case it is about −53 Wm^{-2}. The negative sign indicates a flux out of the ocean, representing a net heat loss from the ocean. Hence, the surface fluxes tend to cool the ocean more in the "wet" case compared to the "dry" case and cannot explain the relative warming in the "wet" case. To more clearly understand the role of oceanic mixing, we construct probability distribution functions (PDFs) of MLD change induced by TCs (Figure S2 in Supporting Information S1). Compared to the PDF for the "Dry" case, the PDF for the "Wet" case is shifted to the left, indicating lower values of MLD changes. Further, the mean TC-induced MLD deepening is 4.3 m less for the "Wet" case

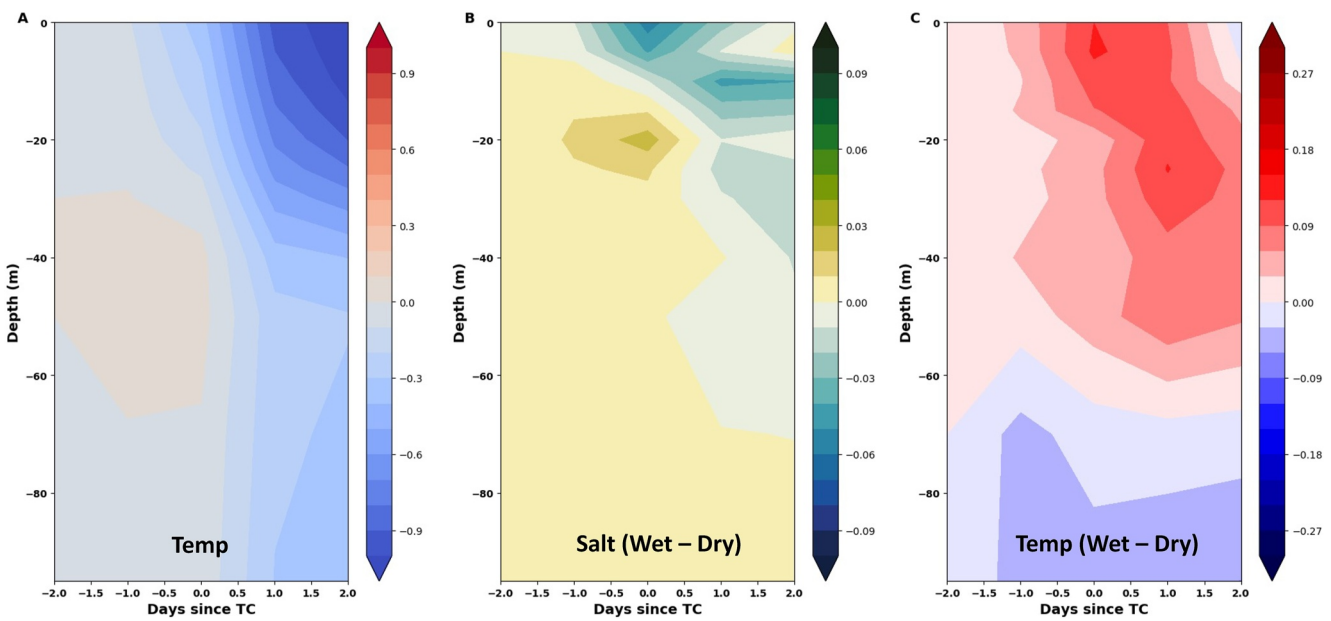

Figure 2. (a) Composite mean anomalous upper-ocean temperature response to tropical cyclones (TCs) (°C). Difference in composite mean anomalous upper ocean (b) salinity (psu), and (c) temperature (°C) response to TCs between the "wet" and "dry" cases. The temperature and salinity profiles are averaged over a 2° × 2° box centered over the storm. These results are based on 20 years of high-resolution Energy Exascale Earth System Model simulations. "Anomalous" here refers to the deviation from the prestorm state and "composite mean" indicates averaging across all wet/dry cases.

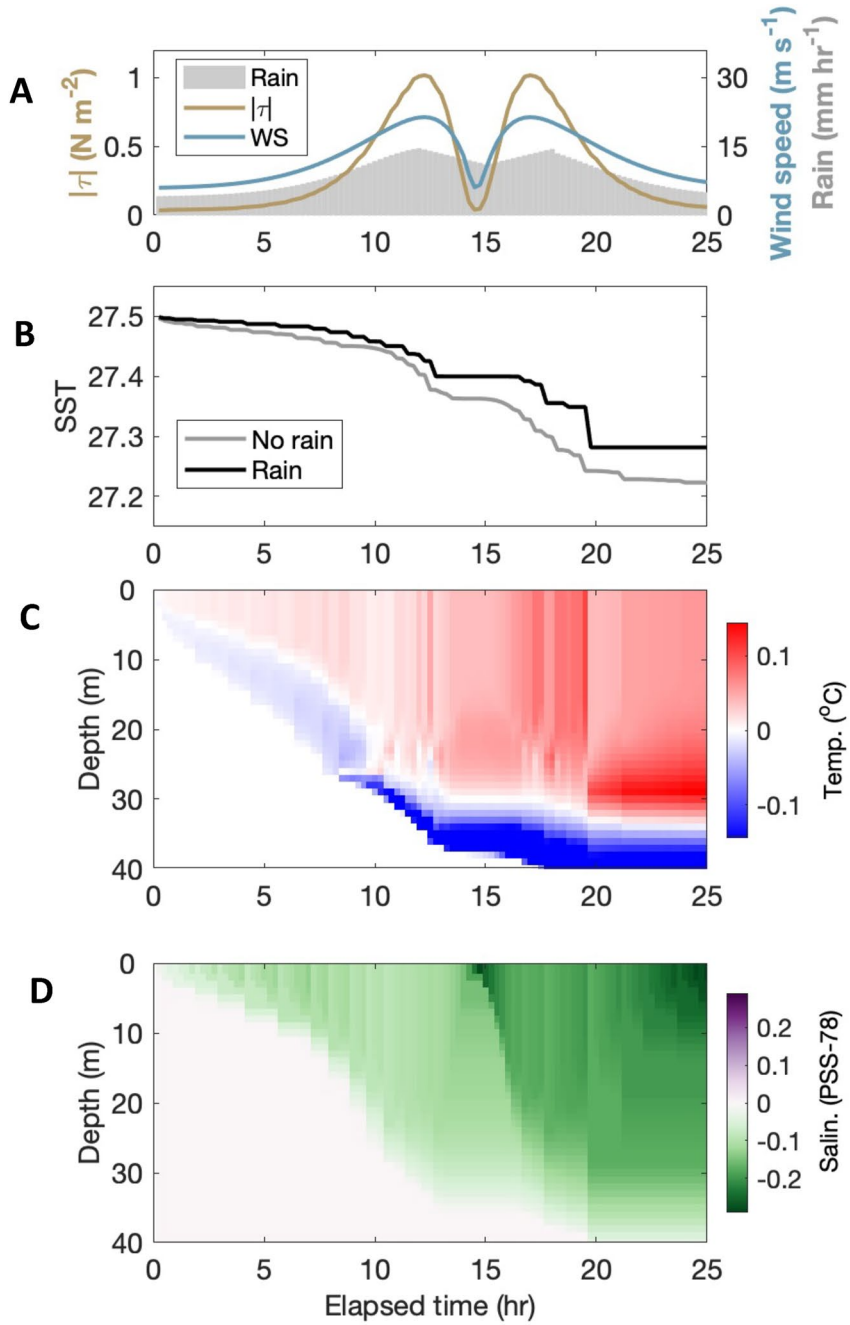

Figure 3. (a) Profiles of surface wind speed (m s^{-1}), wind stress (N m^{-2}), and rainfall (mm hr^{-1}) used as forcing for the Price-Weller-Pinkel ocean mixed layer model. While the wind forcing is common to both the "Rain" and "No rain" experiments, the rainfall profile was only applied to the "Rain" experiment. (b) Time evolution of sea surface temperature (°C) in the "Rain" and "No rain" cases. Difference in time evolution of (c) temperature (°C) and (d) salinity (psu) between the "Rain" and "No rain" cases.

compared to the "Dry" case. This suggests that the freshening at the ocean surface reduces mechanical mixing, enhances salinity stratification, and decreases sea surface cooling.

To more clearly delineate the role of oceanic mixing in the rainfall-induced SST response to TCs, we performed numerical sensitivity experiments using the PWP model (Price et al., 1986) with idealized TC forcing (Figure 3a). In the two experiments, the TC forcing is identical except that the "No rain" case does not include rainfall, while the "Rain" case includes rainfall. The rain rate and near-surface wind speed both reach maxima near the eye of the

storm (Figure 3a). The time evolution of SST in the two experiments (Figure 3b) reveals that the surface temperatures closely follow each other until the first passage of the eyewall at about 12 hr. Subsequently, the SST in the "Rain" experiment decreases less than the SST in the "No rain" experiment. The initial and final vertical temperature profiles (Figure S3a in Supporting Information S1) indicate that the SST cooling in the "Rain" case is reduced by about 0.07°C compared to the "No rain" case. There is less cooling of the ocean approximately in the upper 30 m and more cooling below in the "Rain" case (Figure 3c). This is in good agreement with the relative freshening of the ocean in the "Rain" case that is confined to an approximate depth of 30 m (Figure 3d). These idealized numerical experiments reinforce the results obtained previously from observations and high-resolution climate model simulations.

4. Summary and Discussion

Using a combination of observations, simulations from a high-resolution climate model, and idealized numerical sensitivity experiments using an ocean mixed layer model, we demonstrate that rainfall under TCs can play a role in the sea surface cooling induced by them. When TCs produce a large amount of rainfall, the upper ocean freshens significantly, increasing density stratification. This reduces the SST cooling induced by the storm, weakening mixing and entrainment at the base of the mixed layer. While the impact of rainfall on TC-induced SST cooling has mostly been neglected previously, our study suggests that rainfall can play an active role in air-sea interactions for weaker TCs. The reduction in the magnitude of TC-induced SST cooling by TC rainfall was higher in observations and climate model simulations than in the idealized ocean mixed layer model simulations. This likely suggests that although vertical ocean mixing does appear to play a role, other subsurface ocean processes such as Ekman upwelling and horizontal advection may also be responsible for rainfall's impact on SST cooling, in addition to a potential minor contribution from surface fluxes. Note that the temperature of the rain drops has a negligible effect on the modulation of SST change (Jourdain et al., 2013). Further, we considered area-averaged parameters in our composite-based analysis, which could lead to underestimation of certain coupled processes. Controlled numerical experiments with high-resolution numerical models at cloud-resolving resolution could potentially help address this issue.

In our study, we subsampled data to ensure a fair comparison between distributions with high and low rain rates. However, due to this process, we could only consider weaker storms. Thus, one wonders whether similar impacts of rainfall are possible at higher wind speeds. To explore this, we performed a set of numerical experiments with the PWP model by increasing the intensity of the TC from 35 to 100 kt for varying ocean initial conditions, which include the initial MLD and temperature stratification beneath the mixed layer (Figure S4 in Supporting Information S1). In general, the reduction in SST cooling due to rainfall is more prominent for weaker storms with smaller MLDs (Figure S4a in Supporting Information S1) and higher temperature stratification (Figure S4b in Supporting Information S1), since the SST cooling induced by a TC varies inversely with the MLD and directly with temperature stratification (Price, 1981). Interestingly, as TC intensity increases, the reduction in SST cooling by rain increases initially and decreases subsequently. For instance, when we consider the simulations with varying MLDs, the maximum impact of rainfall occurs for wind speeds between approximately 50 and 70 kt (Figure S4a in Supporting Information S1). This is because at low wind speeds, wind-induced mixing is weak and hence changes in stratification play a smaller role in the upper-ocean response to TCs (Balaguru, Foltz, et al., 2020). On the other hand, at high wind speeds, wind-induced mixing is very strong and overwhelms the relatively weak effect of TC rainfall. Thus, the process demonstrated in this study may also be relevant for TCs with higher intensities (up to 70 kt) than those considered in our analysis. Modulation of the wind mixing-SST cooling relationship by rainfall (Figure S4a in Supporting Information S1) may also be relevant for TCs of Category 3 and of higher strength. For instance, rainfall may impact sea surface cooling away from the cores of intense TCs depending on how the winds and rainfall are distributed spatially, and it may also affect the right-left asymmetry in SST cooling along storm tracks (Steffen & Bourassa, 2020).

Since TC-induced SST cooling plays a critical role in TC intensification, rainfall from TCs could potentially act as a positive feedback mechanism for storms, especially for TCs that are in the weaker stages of their life cycles and rain more. This has substantial implications for studies focused on improving our understanding of TC intensification and the representation of TCs in coupled and uncoupled models. Finally, TC rain rates are projected to rise under global warming (Guzman & Jiang, 2021; Tu et al., 2021) with an amplification of the hydrological cycle. A simple sensitivity experiment with a doubling of the TC rain rate suggests that the reduction in SST

cooling caused by rainfall could increase (Figure S5 in Supporting Information S1). Hence, we speculate that the mechanism identified in our study may play an increasingly important role in TC intensification as the planet warms.

Conflict of Interest

The authors declare no conflicts of interest relevant to this study.

Data Availability Statement

The sources for various observational data used in this study are as follows: Tropical cyclone track data (https://www.ncdc.noaa.gov/ibtracs/), Global Precipitation Climatology Project daily precipitation data (http://doi.org/10.7289/V5RX998Z), Tropical Rainfall Measuring Mission 3-hourly precipitation data (https://doi.org/10.5067/TRMM/TMPA/3H/7), NOAA daily optimum interpolation sea surface temperature (SST) data (https://www.ncei.noaa.gov/data/sea-surface-temperature-optimum-interpolation/), Tropical Microwave Imager SST data (www.remss.com/missions/tmi), and Simple Ocean Data Assimilation version 3.3.1 5-day mean vertical profiles of ocean temperature and salinity (https://www.soda.umd.edu/). The Energy Exascale Earth System Model model data used in this study is available at https://esgf-node.llnl.gov/search/e3sm/. The source code for the Price-Weller-Pinkel ocean model is available at http://www.po.gso.uri.edu/rafos/research/pwp/.

Acknowledgments
K. Balaguru, L. R. Leung, and S. M. Hagos are supported by the Office of Science (BER) of the U.S. Department of Energy as part of the Regional and Global Model Analysis program area through the Water Cycle and Climate Extremes Modeling project and the collaborative multiprogram Integrated Coastal Modeling project. The Pacific Northwest National Laboratory is operated for DOE by Battelle Memorial Institute under contract no. DE-AC05-76RL01830. G. R. Foltz was funded by base funds to NOAA/AOML's Physical Oceanography Division. The computations were mainly carried out using the computing resources at the National Energy Research Scientific Computing Center, a U.S. Department of Energy Office of Science User Facility located at Lawrence Berkeley National Laboratory, operated under contract no. DE-AC02-05CH11231.

References

Balaguru, K., Chang, P., Saravanan, R., Leung, L. R., Xu, Z., Li, M., & Hsieh, J.-S. (2012). Ocean barrier layers' effect on tropical cyclone intensification. *Proceedings of the National Academy of Sciences*, *109*(36), 14343–14347. https://doi.org/10.1073/pnas.1201364109

Balaguru, K., Foltz, G. R., Leung, L. R., Asaro, E. D., Emanuel, K. A., Liu, H., & Zedler, S. E. (2015). Dynamic potential intensity: An improved representation of the ocean's impact on tropical cyclones. *Geophysical Research Letters*, *42*(16), 6739–6746. https://doi.org/10.1002/2015gl064822

Balaguru, K., Foltz, G. R., Leung, L. R., Kaplan, J., Xu, W., Reul, N., & Chapron, B. (2020). Pronounced impact of salinity on rapidly intensifying tropical cyclones. *Bulletin of the American Meteorological Society*, *101*(9), E1497–E1511. https://doi.org/10.1175/bams-d-19-0303.1

Balaguru, K., Leung, L. R., Van Roekel, L. P., Golaz, J.-C., Ullrich, P. A., Caldwell, P. M., et al. (2020). Characterizing tropical cyclones in the energy exascale Earth system model Version 1. *Journal of Advances in Modeling Earth Systems*, *12*(8), e2019MS002024. https://doi.org/10.1029/2019ms002024

Balaguru, K., Leung, L. R., & Yoon, J.-h. (2013). Oceanic control of northeast Pacific hurricane activity at interannual timescales. *Environmental Research Letters*, *8*(4), 044009. https://doi.org/10.1088/1748-9326/8/4/044009

Bell, R., Strachan, J., Vidale, P. L., Hodges, K., & Roberts, M. (2013). Response of tropical cyclones to idealized climate change experiments in a global high-resolution coupled general circulation model. *Journal of Climate*, *26*(20), 7966–7980. https://doi.org/10.1175/jcli-d-12-00749.1

Bender, M. A., & Ginis, I. (2000). Real-case simulations of hurricane–ocean interaction using a high-resolution coupled model: Effects on hurricane intensity. *Monthly Weather Review*, *128*(4), 917–946. https://doi.org/10.1175/1520-0493(2000)128<0917:rcsoho>2.0.co;2

Caldwell, P. M., Mametjanov, A., Tang, Q., Van Roekel, L. P., Golaz, J.-C., Lin, W., et al. (2019). The DOE E3SM coupled model version 1: Description and results at high resolution. *Journal of Advances in Modeling Earth Systems*, *11*(12), 4095–4146. https://doi.org/10.1029/2019ms001870

Carton, J. A., Chepurin, G. A., & Chen, L. (2018). SODA3: A new ocean climate reanalysis. *Journal of Climate*, *31*(17), 6967–6983. https://doi.org/10.1175/jcli-d-18-0149.1

Cione, J. J., & Uhlhorn, E. W. (2003). Sea surface temperature variability in hurricanes: Implications with respect to intensity change. *Monthly Weather Review*, *131*(8), 1783–1796. https://doi.org/10.1175//2562.1

D'Asaro, E. A., Sanford, T. B., Niiler, P. P., & Terrill, E. J. (2007). Cold wake of hurricane Frances. *Geophysical Research Letters*, *34*(15). https://doi.org/10.1029/2007gl030160

DeMaria, M. (1987). Tropical cyclone track prediction with a barotropic spectral model. *Monthly Weather Review*, *115*(10), 2346–2357. https://doi.org/10.1175/1520-0493(1987)115<2346:tctpwa>2.0.co;2

DeMaria, M., & Kaplan, J. (1994). Sea surface temperature and the maximum intensity of Atlantic tropical cyclones. *Journal of Climate*, *7*(9), 1324–1334. https://doi.org/10.1175/1520-0442(1994)007<1324:sstatm>2.0.co;2

Emanuel, K., DesAutels, C., Holloway, C., & Korty, R. (2004). Environmental control of tropical cyclone intensity. *Journal of the Atmospheric Sciences*, *61*(7), 843–858. https://doi.org/10.1175/1520-0469(2004)061<0843:ecotci>2.0.co;2

Emanuel, K. A. (1986). An air-sea interaction theory for tropical cyclones. Part I: Steady-state maintenance. *Journal of the Atmospheric Sciences*, *43*(6), 585–605. https://doi.org/10.1175/1520-0469(1986)043<0585:aasitf>2.0.co;2

Emanuel, K. A. (1999). Thermodynamic control of hurricane intensity. *Nature*, *401*(6754), 665–669. https://doi.org/10.1038/44326

Gentemann, C. L., Wentz, F. J., Mears, C. A., & Smith, D. K. (2004). In situ validation of Tropical Rainfall Measuring Mission microwave sea surface temperatures. *Journal of Geophysical Research*, *109*(C4), C04021. https://doi.org/10.1029/2003jc002092

Grodsky, S. A., Reul, N., Lagerloef, G., Reverdin, G., Carton, J. A., Chapron, B., et al. (2012). Haline hurricane wake in the Amazon/Orinoco plume: AQUARIUS/SACD and SMOs observations. *Geophysical Research Letters*, *39*(20), 2012GL053335. https://doi.org/10.1029/2012gl053335

Guzman, O., & Jiang, H. (2021). Global increase in tropical cyclone rain rate. *Nature Communications*, *12*(1), 1–8. https://doi.org/10.1038/s41467-021-25685-2

Haarsma, R. J., Roberts, M. J., Vidale, P. L., Senior, C. A., Bellucci, A., Bao, Q., et al. (2016). High resolution model intercomparison project (HighResMIP v1. 0) for CMIP6. *Geoscientific Model Development*, *9*(11), 4185–4208. https://doi.org/10.5194/gmd-9-4185-2016

Hlywiak, J., & Nolan, D. S. (2019). The influence of oceanic barrier layers on tropical cyclone intensity as determined through idealized, coupled numerical simulations. *Journal of Physical Oceanography*, *49*(7), 1723–1745. https://doi.org/10.1175/jpo-d-18-0267.1

Holland, G. J. (1997). The maximum potential intensity of tropical cyclones. *Journal of the Atmospheric Sciences*, *54*(21), 2519–2541. https://doi.org/10.1175/1520-0469(1997)054<2519:tmpiot>2.0.co;2

Hsu, S., & Yan, Z. (1998). A note on the radius of maximum wind for hurricanes. *Journal of Coastal Research*, *14*(2).

Huffman, G. J., Adler, R. F., Morrissey, M. M., Bolvin, D. T., Curtis, S., Joyce, R., et al. (2001). Global precipitation at one-degree daily resolution from multisatellite observations. *Journal of Hydrometeorology*, *2*(1), 36–50. https://doi.org/10.1175/1525-7541(2001)002<0036:gpaodd>2.0.co;2

Jourdain, N. C., Lengaigne, M., Vialard, J., Madec, G., Menkes, C. E., Vincent, E. M., et al. (2013). Observation-based estimates of surface cooling inhibition by heavy rainfall under tropical cyclones. *Journal of Physical Oceanography*, *43*(1), 205–221. https://doi.org/10.1175/jpo-d-12-085.1

Knapp, K. R., Kruk, M. C., Levinson, D. H., Diamond, H. J., & Neumann, C. J. (2010). The international best track archive for climate stewardship (IBTrACS) unifying tropical cyclone data. *Bulletin of the American Meteorological Society*, *91*(3), 363–376. https://doi.org/10.1175/2009bams2755.1

Korty, R. L., Emanuel, K. A., & Scott, J. R. (2008). Tropical cyclone–induced upper-ocean mixing and climate: Application to equable climates. *Journal of Climate*, *21*(4), 638–654. https://doi.org/10.1175/2007jcli1659.1

Lin, I., Wu, C.-C., Emanuel, K. A., Lee, I.-H., Wu, C.-R., & Pun, I.-F. (2005). The interaction of Supertyphoon Maemi (2003) with a warm ocean eddy. *Monthly Weather Review*, *133*(9), 2635–2649. https://doi.org/10.1175/mwr3005.1

Lin, I.-I., Black, P., Price, J. F., Yang, C.-Y., Chen, S. S., Lien, C.-C., et al. (2013). An ocean coupling potential intensity index for tropical cyclones. *Geophysical Research Letters*, *40*(9), 1878–1882. https://doi.org/10.1002/grl.50091

Lin, Y., Zhao, M., & Zhang, M. (2015). Tropical cyclone rainfall area controlled by relative sea surface temperature. *Nature Communications*, *6*(1), 1–7. https://doi.org/10.1038/ncomms7591

Liu, F., Zhang, H., Ming, J., Zheng, J., Tian, D., & Chen, D. (2020). Importance of precipitation on the upper ocean salinity response to typhoon kalmaegi (2014). *Water*, *12*(2), 614. https://doi.org/10.3390/w12020614

Mainelli, M., DeMaria, M., Shay, L. K., & Goni, G. (2008). Application of oceanic heat content estimation to operational forecasting of recent Atlantic category 5 hurricanes. *Weather and Forecasting*, *23*(1), 3–16. https://doi.org/10.1175/2007waf2006111.1

Morey, S. L., Bourassa, M. A., Dukhovskoy, D. S., & O'Brien, J. J. (2006). Modeling studies of the upper ocean response to a tropical cyclone. *Ocean Dynamics*, *56*(5), 594–606. https://doi.org/10.1007/s10236-006-0085-y

Price, J. F. (1981). Upper ocean response to a hurricane. *Journal of Physical Oceanography*, *11*(2), 153–175. https://doi.org/10.1575/1912/10271

Price, J. F. (2009). Metrics of hurricane-ocean interaction: Vertically-integrated or vertically-averaged ocean temperature? *Ocean Science*, *5*(3), 351–368. https://doi.org/10.5194/os-5-351-2009

Price, J. F., Weller, R. A., & Pinkel, R. (1986). Diurnal cycling: Observations and models of the upper ocean response to diurnal heating, cooling, and wind mixing. *Journal of Geophysical Research*, *91*(C7), 8411–8427. https://doi.org/10.1029/jc091ic07p08411

Reul, N., Chapron, B., Grodsky, S. A., Guimbard, S., Kudryavtsev, V., Foltz, G. R., & Balaguru, K. (2021). Satellite observations of the sea surface salinity response to tropical cyclones. *Geophysical Research Letters*, *48*(1), e2020GL091478. https://doi.org/10.1029/2020gl091478

Reul, N., Quilfen, Y., Chapron, B., Fournier, S., Kudryavtsev, V., & Sabia, R. (2014). Multisensor observations of the A mazon-O rinoco river plume interactions with hurricanes. *Journal of Geophysical Research: Oceans*, *119*(12), 8271–8295. https://doi.org/10.1002/2014jc010107

Reynolds, R. W., Smith, T. M., Liu, C., Chelton, D. B., Casey, K. S., & Schlax, M. G. (2007). Daily high-resolution-blended analyses for sea surface temperature. *Journal of Climate*, *20*(22), 5473–5496. https://doi.org/10.1175/2007jcli1824.1

Roemmich, D., Johnson, G. C., Riser, S., Davis, R., Gilson, J., Owens, W. B., et al. (2009). The Argo Program: Observing the global ocean with profiling floats. *Oceanography*, *22*(2), 34–43. https://doi.org/10.5670/oceanog.2009.36

Rudzin, J. E., Shay, L. K., & Jaimes de la Cruz, B. (2019). The impact of the Amazon–Orinoco River plume on enthalpy flux and air–sea interaction within Caribbean Sea tropical cyclones. *Monthly Weather Review*, *147*(3), 931–950. https://doi.org/10.1175/mwr-d-18-0295.1

Rudzin, J. E., Shay, L. K., & Johns, W. E. (2018). The influence of the barrier layer on SST response during tropical cyclone wind forcing using idealized experiments. *Journal of Physical Oceanography*, *48*(7), 1471–1478. https://doi.org/10.1175/jpo-d-17-0279.1

Schade, L. R., & Emanuel, K. A. (1999). The ocean's effect on the intensity of tropical cyclones: Results from a simple coupled atmosphere–ocean model. *Journal of the Atmospheric Sciences*, *56*(4), 642–651. https://doi.org/10.1175/1520-0469(1999)056<0642:toseot>2.0.co;2

Shay, L. K., Goni, G. J., & Black, P. G. (2000). Effects of a warm oceanic feature on Hurricane Opal. *Monthly Weather Review*, *128*(5), 1366–1383. https://doi.org/10.1175/1520-0493(2000)128<1366:eoawof>2.0.co;2

Shen, W., & Ginis, I. (2003). Effects of surface heat flux-induced sea surface temperature changes on tropical cyclone intensity. *Geophysical Research Letters*, *30*(18), 1933. https://doi.org/10.1029/2003gl017878

Steffen, J., & Bourassa, M. (2020). Upper-ocean response to precipitation forcing in an ocean model hindcast of hurricane Gonzalo. *Journal of Physical Oceanography*, *50*(11), 3219–3234. https://doi.org/10.1175/jpo-d-19-0277.1

Tu, S., Xu, J., Chan, J. C., Huang, K., Xu, F., & Chiu, L. S. (2021). Recent global decrease in the inner-core rain rate of tropical cyclones. *Nature Communications*, *12*(1), 1–9. https://doi.org/10.1038/s41467-021-22304-y

Ullrich, P. A., & Zarzycki, C. M. (2017). Tempestextremes: A framework for scale-insensitive pointwise feature tracking on unstructured grids. *Geoscientific Model Development*, *10*(3), 1069–1090. https://doi.org/10.5194/gmd-10-1069-2017

Vincent, E. M., Emanuel, K. A., Lengaigne, M., Vialard, J., & Madec, G. (2014). Influence of upper ocean stratification interannual variability on tropical cyclones. *Journal of Advances in Modeling Earth Systems*, *6*(3), 680–699. https://doi.org/10.1002/2014ms000327

Vincent, E. M., Lengaigne, M., Vialard, J., Madec, G., Jourdain, N. C., & Masson, S. (2012). Assessing the oceanic control on the amplitude of sea surface cooling induced by tropical cyclones. *Journal of Geophysical Research*, *117*(C5), C05023. https://doi.org/10.1029/2011jc007705

Wentz, F. J., Gentemann, C., Smith, D., & Chelton, D. (2000). Satellite measurements of sea surface temperature through clouds. *Science*, *288*(5467), 847–850. https://doi.org/10.1126/science.288.5467.847

Zeng, L., & Wang, D. (2017). Seasonal variations in the barrier layer in the South China Sea: Characteristics, mechanisms and impact of warming. *Climate Dynamics*, *48*(5–6), 1911–1930. https://doi.org/10.1007/s00382-016-3182-8

Zhang, H., He, H., Zhang, W.-Z., & Tian, D. (2021). Upper ocean response to tropical cyclones: A review. *Geoscience Letters*, *8*(1), 1–12. https://doi.org/10.1186/s40562-020-00170-8

Zhang, W., Villarini, G., Scoccimarro, E., Roberts, M., Vidale, P. L., Vanniere, B., et al. (2021). Tropical cyclone precipitation in the HighResMIP atmosphere-only experiments of the PRIMAVERA project. *Climate Dynamics*, *57*(1–2), 1–21. https://doi.org/10.1007/s00382-021-05707-x